microplastics

MDPI

Article

The Exposure to Polypropylene Micro- and Nanoplastics Impairs Wound Healing and Tissue Regeneration in the Leech *Hirudo verbana*

Camilla Bon [1], Alice Maretti [1], Laura Pulze [1], Nicolò Paris [1], Orlando Santoro [1], Stefania Pragliola [2], Lorella Izzo [1], Nicolò Baranzini [1,*] and Annalisa Grimaldi [1,*]

[1] Department of Biotechnology and Life Sciences, University of Insubria, Via J.H. Dunant 3, 21100 Varese, Italy; cbon@uninsubria.it (C.B.); alice.maretti1@gmail.com (A.M.); laura.pulze@uninsubira.it (L.P.); nparis@studenti.uninsubria.it (N.P.); orlando.santoro@uninsubria.it (O.S.); lorella.izzo@uninsubria.it (L.I.)

[2] Department of Chemistry and Biology, University of Salerno and INSTM Research Unit, Via Giovanni Paolo II 132, 84084 Fisciano, Italy; spragliola@unisa.it

* Correspondence: nicolo.baranzini@uninsubria.it (N.B.); annalisa.grimaldi@uninsubria.it (A.G.); Tel.: +39-0332-421325 (A.G.)

Abstract

Plastic pollution represents a persistent global issue, with catastrophic effects on ecosystems. Due to unique properties, these synthetic materials do not break down into biodegradable compounds when naturally dispersed, but degrade into smaller fragments, known as micro- (MPs) and nanoplastics (NPs), that easily enter the food chain. Among plastics, polypropylene (PP) is one of the most common, whose consumption has dramatically increased in recent years for single-use packaging and surgical masks. In this context, given the widespread detection of PP-MPs and NPs in various biological matrices, investigating their toxicity in living organisms is crucial. For these reasons, this study aims to assess how PP-MPs and NPs affect tissue regeneration following injury, proposing the freshwater leech *Hirudo verbana* as an established experimental model. Injured leeches were examined at different time points after plastic administration, and analyses were conducted using microscopy, immunofluorescence, and molecular biology techniques. The results demonstrate that plastic exposure induces fibrosis, disrupts tissue reorganization, delays wound repair, and activates the innate immune and oxidative stress responses. In summary, this project provides new insight into the adverse effects of PP particles on living organisms, highlighting for the first time their negative impact on proper tissue regeneration.

Keywords: plastic pollution; polypropylene; innate immune response; chronic inflammation; wound healing

check for updates

Academic Editor: Nicolas Kalogerakis

Received: 29 July 2025
Revised: 14 August 2025
Accepted: 16 August 2025
Published: 27 August 2025

Citation: Bon, C.; Maretti, A.; Pulze, L.; Paris, N.; Santoro, O.; Pragliola, S.; Izzo, L.; Baranzini, N.; Grimaldi, A. The Exposure to Polypropylene Micro- and Nanoplastics Impairs Wound Healing and Tissue Regeneration in the Leech *Hirudo verbana*. *Microplastics* **2025**, *4*, 56. https://doi.org/10.3390/microplastics4030056

Copyright: © 2025 by the authors. Licensee MDPI, Basel, Switzerland. This article is an open access article distributed under the terms and conditions of the Creative Commons Attribution (CC BY) license (https://creativecommons.org/licenses/by/4.0/).

1. Introduction

Due to the unique properties, such as high versatility and robustness, plastics take up a fundamental role in modern society, finding a place in a wide range of both civil and manufacturing applications. Among the different types of synthetic polymers, polyethylene terephthalate (PET), polypropylene (PP), polystyrene (PS), low- and high-density polyethylene (LDPE and HDPE) and polyvinyl chloride (PVC) are certainly the most diffused and also the most used worldwide. However, although plastic production changed our life, its large consumption leads to an incessant release, with millions of tons reverse into the environment every year, and that very often constitutes the predominant pollutant [1,2].

For this reason, the impact on the biological matrices and the resulting effects on living organisms represent the most discussed issues worldwide, as well as finding new solutions to limit the dispersion. In particular, the chemical bonds that compose these polymers not only make these materials extremely resilient but also impervious to natural degradation [3]. Indeed, rather than decomposing into molecular or further biodegradable elements, plastic waste degrades into smaller particles under the action of abiotic and biotic factors, known as micro- (MPs) and nanoplastics (NPs), which have been found in different shapes and that can be easily dispersed by natural events [4].

Currently, it is estimated that 80% of the plastics found in the oceans originate from land sources, with rivers being the major pathways to marine waters [5]. Although the effects of plastics in marine environments have received substantial attention, it is equally crucial to investigate their impacts on freshwater ecosystems. Not only are urban centers often localized in proximity to rivers, lakes, and waterways, but these are also vital for maintaining biodiversity, supplying drinking water, and supporting agricultural or industrial activities [5,6]. Additionally, freshwater habitats host a wide variety of animal species, many of which depend on these ecosystems for their entire life cycles or also for essential developmental stages. Thus, the introduction of plastic pollutants not only affects their survival, interfering with the main biological processes, causing toxic effects, but also leads to a continuous absorption with the subsequent entry into the food chain.

Indeed, recent studies have shown that microplastics and synthetic fibers can induce acute and chronic toxicity in freshwater invertebrates such as *Hyalella azteca* and *Daphnia magna*, with effects influenced by exposure duration, particle type, and morphology [7,8]. When ingested, MPs and NPs bioaccumulate in larger quantities, with the potential risk of also reaching humans and inducing a range of health problems. Moreover, one of the primary concerns is that this plastic debris can absorb and carry harmful chemicals, such as pesticides, heavy metals, and persistent organic pollutants [9].

In this context, among the most diffused plastics found in freshwaters, polypropylene (PP) constitutes 24% of the whole [10]. Compared to other compounds, this polymer possesses the lowest density and the highest melting temperature and chemical inertness, all properties that make it highly versatile and optimum for long-life applications [11,12]. Accordingly, it has always been considered the ideal choice to produce flexible, long-lasting, cheap, and light plastics used for packaging, for producing common commercial (e.g., bags, bottle caps, food containers) or medical (e.g., surgical masks) items [11,13]. Obviously, like the other plastics, given its long-term persistence and bioaccumulation ability, PP also represents a challenge in terms of the environment [14–16]. Several studies have been devoted to understanding the biological effects following PP plastic exposure in both terrestrial and aquatic animals, such as rodents, fish, crustaceans, annelids, molluscs, echinoderms, nematodes, and cnidarians [17]. It has been demonstrated that PP-MPs and NPs generate inflammation, not only increasing the number of immune cells but also inducing lipid peroxidation, with consequent production of reactive oxygen species (ROS), and upregulating the expression of several cytokines and antioxidant enzymes [18,19]. Moreover, the presence of particles alters the composition and the diversity of the gut microbiome, with perturbation of the bacterial community and the increase of harmful microorganisms, both in vertebrates [18] and invertebrates [20].

Contrariwise, to date, there are no studies in the literature concerning the PP effects on tissue regeneration. Although several analyses have been conducted for other plastic types, no data are available on PP-MPs and NPs. Indeed, it has been observed that in the planarian model *Dugesia japonica*, small spheres or short fibers of PE/PET induced a significant reduction in body and blastema size, reflecting a reduced growth rate and weakening regenerative capabilities [21]. Similarly, PS-MPs caused a reduction of the

blastema area in a dose-dependent manner, with the suppression of apoptotic activity and the inhibition of planarian stem cell proliferation [22]. Among annelids, in the polychaeta *Perinereis aibuhitensis*, an important commercial specie in Asia, it was demonstrated that after segment amputation the exposure of PS-MPs hinders the posterior segment regeneration [23].

Based on these premises, in order to evaluate how PP-MPs and NPs could interfere with the correct tissue regeneration during wound healing, in the present study, the *Hirudo verbana* medicinal leech has been proposed as a freshwater experimental animal model. Interestingly, previous studies have already demonstrated the validity of this invertebrate in assessing the effects of PP-MPs and NPs that, upon being internalized inside tissues, caused inflammation, innate immune response activation and increased expression of several antioxidant enzymes [19]. Specifically, here, leeches have been injured and subsequently exposed to PP-MPs and NPs for different timings, which have been resuspended in water tanks to mimic the heterogeneous and natural behavior of these particles. The data collected show that the presence of plastics impairs the regular reorganization of tissues, inducing fibrosis in exposed animals. Indeed, PP-MPs and NPs not only induce an increase in both immune cells and fibroblast numbers, but also lead to an excessive expression of genes involved in this specific process, such as Smad3 and TGF-β, with consequent abundant production of collagen I. In addition, this excess of extracellular matrix impairs the correct formation of new blood vessels, which are fundamental to recruit CD34-positive precursor cells in the wound healing area.

This study not only confirms as the leech *H. verbana* represents a valuable complementary model to evaluate the possible harmful effects of pollutants on living organisms, with the possibility to transfer the information obtained to vertebrates but also show for the first time that the presence of plastics particles affects the regular reorganization of tissues after injury, interfering both with the immune system and the regenerative mechanism.

2. Materials and Methods

2.1. Preparation and Characterization of PP-MPs and NPs by Means of Transmission Electron Microscopy (TEM)

Similarly to a previously reported procedure [24], 4 mL of MAO solution (toluene, 10 wt %, purchased from Sigma-Aldrich, Milan, Italy) was diluted in 48 mL of dry toluene (purchased from Sigma-Aldrich, refluxed over sodium for 48 h and distilled before use) in a 250 mL round bottom flask equipped with a magnetic stirrer under an inert atmosphere (N_2) at room temperature (20 °C). The N_2 atmosphere was removed from the reaction flask, and a constant propylene overpressure was applied to the solution. After 5 min, polymerization was started by introducing 8 mL of dry toluene solution of *rac*-[$(CH_3)_2$Si(indenyl)$_2$]$ZrCl_2$ (28.0 mg, 0.0624 mmol, purchased from Strem Chemicals, Inc.). Polymerization was stopped after 20 min by introducing a few milliliters of ethanol. Then, the polypropylene (PP) was coagulated in excess of acidified ethanol, washed several times with fresh ethanol and dried in a vacuum at room temperature. In this study, the polymer fraction soluble in toluene (M_n = 25 kDa, $Đ$ = 2.2, determined by SEC analysis) was used. It was obtained after polymer extraction carried out with boiling acetone and subsequently by boiling toluene using a Kumagawa extractor. Polymer stereoregularity degree, measured in terms of pentades *mmmm* by ^{13}C NMR spectroscopy, was 97%. T_d = 395 °C (5% weight loss), T_m = 140 °C. Full details of polypropylene characterization, including ^{13}C NMR spectroscopy, X-ray diffraction (XRD), thermal analysis, and molecular weight determination, are provided in the Supplementary Materials (Figures S1–S5). Polymer films were obtained by casting from PP solutions in toluene (1 g/50 mL) were formed starting from synthetized polypropylene (PP) films previously dried in a vacuum and then frozen

with liquid nitrogen (−196 °C), and ground in a mortar, to better simulate environmental fragmentation and to obtain a heterogeneous composition in the range between 5 µm and 100 nm. Subsequently, 10 µL of the obtained PP-MPs and NPs were resuspended in ethanol and transferred onto copper 300 mesh formvar-carbon-coated electron microscopy grids (Pacific Grid Tech). The drops of PP-MPs and NPs suspension were allowed to dry directly on the grids, and the resulting samples, with the dried particles deposited, were then observed with a JEOL1400Plus transmission electron microscope (Centro di Ricerca e Trasferimento Tecnologico; CRIETT, University of Insubria; instrument code MIC01). Data were recorded with a MORADA digital camera system (Olympus, Tokyo, Japan) to analyze particle size, morphology, and distribution.

2.2. Animals and Treatments

Adult leeches of the species *H. verbana* (Annelida, kindly donated by ILFARM Srl, Varese, Italy), measuring 10 cm and 1 g in weight, were kept in fresh water (NaCl 1.5 g/L) in aerated tanks at 20 °C. The two experimental conditions reported below (Groups 1 and 2) were performed in triplicate, and a total of five animals were used for each. This sample size was determined based on previous studies in *H. verbana* and *H. medicinalis*, and it is sufficient to obtain statistically representative data while adhering to the 3Rs principles by minimizing the number of animals used.

Group 1: injured and PP-unexposed leeches (n = 15 per group in total), used as a control to evaluate the physiological mechanism of tissue regeneration.

Group 2: injured leeches (n = 15 per group) were exposed by immersion to a 50 mg/L suspension of PP-MPs and NPs prepared with sterilized materials and filtered water. No injections were performed. Tanks and instruments were sterilized before use, and both control and treated groups were kept under identical conditions to minimize microbial interference.

The use of the leech *H. verbana* is not among the animals protected under Directive 2010/63/EU, which governs the use of animals in scientific research, nor is it listed in Legislative Decree no. 26, of 4 March 2014, "Implementing Directive 2010/63/EU on the protection of animals used for scientific purposes", published in the Italian Official Journal on 14 March 2014. However, its use has been approved by the Animal Welfare Body (OPBA) at the University of Insubria, and it complies with the commonly accepted '3Rs.

Before injury induction, leeches were anesthetized by immersion in a 10% ethanol solution in freshwater until complete loss of movement and responsiveness to tactile stimuli. Subsequently, three serial longitudinal incisions, spaced 1 cm apart, were made on the dorsal surface of each animal using a sterile razor blade, transecting the full thickness of the body wall (including the cuticle, epithelium, and all three muscle layers). The first incision was positioned approximately 20 metamers from the posterior end (~1 cm from the posterior sucker). The body of *H. verbana* is anatomically uniform along its entire length. This anatomical consistency ensures that wounds created at this standardized site are fully comparable across all individuals and experimental groups. Animals were then maintained under the assigned experimental conditions and euthanized at 24 h, 48 h, 72 h, and 1 week after the start of treatment, in order to assess their response to the presence of plastic particles. Prior to tissue dissection, animals were euthanized by prolonged immersion in a 10% ethanol solution to ensure irreversible loss of vital functions.

2.3. Embedding Tissue in Epoxy Resin for Morphological Analysis at Light and Transmission Electron Microscopy

As reported in previous works [25], the wounded portion of leeches exposed to PP-MPs and NPs was dissected and fixed in 4% glutaraldehyde diluted in 0.1 M cacodylate buffer (pH 7.4) for 2 h at room temperature. After five washings in the same buffer,

samples were post-fixed in 2% osmium tetroxide (OsO_4) solution for 1 h in the dark at room temperature. Subsequently, tissues were washed in 0.1 M cacodylate buffer, dehydrated with increasing concentrations of ethanol (30%, 50%, 70%, 90%, 96%, 100%), transferred to a solution of propylene oxide and resin (1:1 ratio) for 1 h and finally embedded in an Epon-Araldite 812 mixture epoxy resin (Sigma-Aldrich, Milan, Italy). Sections for light microscopy (0.7 µm in thickness) were obtained with a Reichert Ultracut S ultratome (Leica, Wein, Austria), collected on a slide, and colored with gentian violet (1 g in 100 mL of distilled water) and basic fuchsine (0.13 g in 100 mL of distilled water). Samples were eventually observed under the optical microscope (Eclipse, Nikon, Tokyo, Japan), and the images were captured with the DS-5M-L1 digital camera (Nikon, Tokyo, Japan). From the same samples, ultrathin sections (70 nm in thickness) were obtained with a Reichert Ultracut S ultratome (Leica, Wein, Austria) and were placed on copper grids (300 mesh, Sigma-Aldrich, Milan, Italy), counterstained by uranyl acetate and lead citrate, and analyzed at TEM, as previously described.

2.4. Embedding Tissue in Paraffin and Masson's Trichrome Staining

As previously described [26], tissues were fixed in 4% paraformaldehyde for 2 h and then washed three times in PBS solution (138 mM NaCl, 2.7 mM KCl, 4.3 mM Na_2HPO_4; pH 7.4). Subsequently, samples were dehydrated in an increasing scale of ethanol (30%, 50%, 70%, 90%, 96%, 100%) and finally paraffin-embedded. Sections (7 µm thick) obtained with a rotary microtome (Jung multicut 2045; Leica, Wein, Austria) were processed for Masson's trichrome staining (Bio Optica, Milan, Italy), as suggested by the datasheet. This coloring technique allows us to observe in blue the collagen and the reticular fibers, and in red, the cell cytoplasm. Images were recorded as previously described.

2.5. Embedding Tissue in Oct for Cryosections

The wounded portion of leeches exposed and not to PP-MPs and NPs were dissected, immediately included into OCT (Polyfreeze, TebuBio, Magenta, Italy), frozen in liquid nitrogen and stored at −80 °C. Cryosections (0.7 µm in thickness) were obtained with a cryostat Leica CM1850 (Leica, Wien, Austria), collected on the gelatinated slides, and held at −20 °C.

2.6. Acid Phosphatase (ACP) Assay

Cryosections, obtained as described above, were rehydrated in PBS for 10 min, incubated for 5 min in 0.1 M acetic acid-sodium acetate buffer and then, with the reaction mixture (0.1 M sodium acetate-acetic acid buffer, 0.01% naphthol phosphate, 2% NN-dimethylformamide, 0.06% Fast Red, $MnCl_2$ 0.5 nM) for 90 min, at 37 °C. After several PBS washings, the slides were mounted with Citifluor (Citifluor Ltd., London, UK) and observed under the light microscope.

2.7. Immunolocalizations on Cryosections

The wounded portion of the leeches exposed and not to PP-MPs and NPs has been frozen in OCT as described above. The obtained cryosections were rehydrated for 10 min in PBS buffer and incubated for 30 min in the BSA blocking solution (2% Bovine Serum Albumin, 0.1% Tween diluted in PBS). BSA was also used to dilute antibodies. Samples were incubated for 1 h at room temperature with primary rabbit polyclonal antibody anti-COL1-α2 (Sigma-Aldrich, Milan, Italy), diluted 1:150; rabbit monoclonal anti-CD34 (Abcam, Cambridge, UK), diluted 1:100, already used to detect collagen 1 [26] and HSPCs and myoendothelial cells [27] in leech, respectively. After several washes in PBS buffer, samples were incubated for 45 min at room temperature with secondary antibodies conjugated with fluorescein isothiocyanate (FITC, ThermoFisher Scientific, Milano, Italy, dilution

1:250). The cell nuclei were then counterstained with 4,6-diamidino-2-phenylinedole (DAPI) 0.1 mg/mL diluted in PBS for 5 min, and slides were mounted with PBS/Glycerol Citifluor (Citifluor Ltd., UK). Negative control experiments were performed by omitting primary antibodies. All the samples were examined with the fluorescence microscope (Nikon Digital Sight DS-SM, Tokyo, Japan), and the staining was visualized using excitation/emission filters of 490/525 nm for FITC and 340/488 nm for DAPI. The obtained images were then combined using Adobe Photoshop (Adobe Systems, San Jose, CA, USA).

2.8. RNA Extraction and Quantitative PCR (qPCR)

The proximal regions of the wound of leeches exposed to PP-MPs and NPs were frozen in liquid nitrogen and pestled with a mortar. Samples were then resuspended in 1 mL of TRIzol (Life Technologies, Milano, Italy), centrifuged at 11,270 g for 10 min and then incubated for 5 min at room temperature. Subsequently, 200 µL of chloroform was added, and samples were centrifuged for 15 min at 13,700× *g* at 4 °C. Once the different phases were obtained, 500 µL of the supernatant, in which nucleic acids were present, was recovered and gently mixed with 500 µL of isopropanol. After 10 min at room temperature, samples were centrifuged for 10 min, and the resulting RNA pellets were washed in EtOH 75% and resuspended in DEPC water. Samples were then quantified, and the RNA purity was evaluated with a 1% agarose gel. 2 µg of RNA were retrotranscribed into cDNA using M-MLV reverse transcriptase (Life Technologies, Milano, Italy) in the presence of oligodT (Invitrogen, Thermo Fisher Scientific, Milano, Italy) of random hexamers in a final volume of 20 µL. Quantitative real-time PCR (qPCR) was carried out in triplicate in a CFX Connect Real Time PCR Detection System (Bio-Rad, Milano, Italy) using the iTaq Universal SYBR^{TM} master mix (Bio-Rad, Milano, Italy) and 0.2 µM each forward and reverse primer, in a final volume of 15 µL. The primers used for qPCR amplifications, designed with the web-interface software Primer3Plus [28], have already been tested in previous studies [29] and a list is reported in Table S1 (Supplementary Materials). After initial denaturation, the PCR reaction was performed at 95 °C (10 s), 60 °C (5 s), and 72 °C (10 s) for 39 cycles. Relative gene expressions were calculated using the ΔΔCt method, in which the GAPDH gene (glyceraldehyde-3-phosphate) was used as housekeeping.

2.9. Statistical Analysis

All experiments were conducted in triplicate, and the data show average values ± standard deviations. The fluorescence analysis for immunolocalization approaches was performed using the ImageJ 1.54m software package (https://imagej.net/ij/index.html (accessed on 17 August 2025)) while the statistical analysis was conducted using the Graph Prism 8 software (GraphPad Software, La Jolla, CA, USA; https://www.graphpad.com/features (accessed on 17 August 2025)). The number of fibroblasts and blood vessels was assessed by analyzing 5 different slides, obtained from epoxy resin-embedded samples and stained with gentian violet and basic fuchsine. Images of random fields of 45,000 µm^2 for each slide were taken under the light microscope. The count was performed for each experimental time point using the ImageJ 1.54m software package (https://imagej.net/ij/index.html (accessed on 17 August 2025)). Both the normality and the homoscedasticity of the samples were assessed using the Shapiro-Wilk and the Levene tests. The significant differences were calculated by one-way ANOVA variance analysis, in which a p-value < 0.05 was considered statistically significant following the Tukey post hoc test, and bars represent mean ± standard deviations (SD). In the graphs, the averages with asterisks represent a significant difference between injured leeches not exposed to PP and those exposed to PP-MPs and NPs at different timings. The raw data corresponding to the mean values reported are provided in the Supplementary Files (Tables S2–S10).

3. Results

3.1. Determination of PP-MPs and NPs Presence in Leech Tissues

The heterogeneous mixture of PP-MPs and NPs, obtained by the mechanical grinding of the PP films (as described in the materials and methods chapter), was observed at TEM before performing leech treatments. As reported in the images, the MPs ranged in size between 5 µm and 1 µm (Figure 1a), while that of NPs was around 100 nm (Figure 1b). TEM analyses have also been used to observe the PP-MPs and NPs internalization inside the leech body wall (Figure 1c–f), confirming how, especially nanoparticles, entered inside tissues of exposed animals. Indeed, several NPs aggregates were found, dispersed both underneath the epithelium (Figure 1c,d) and in the injured area (Figure 1e,f).

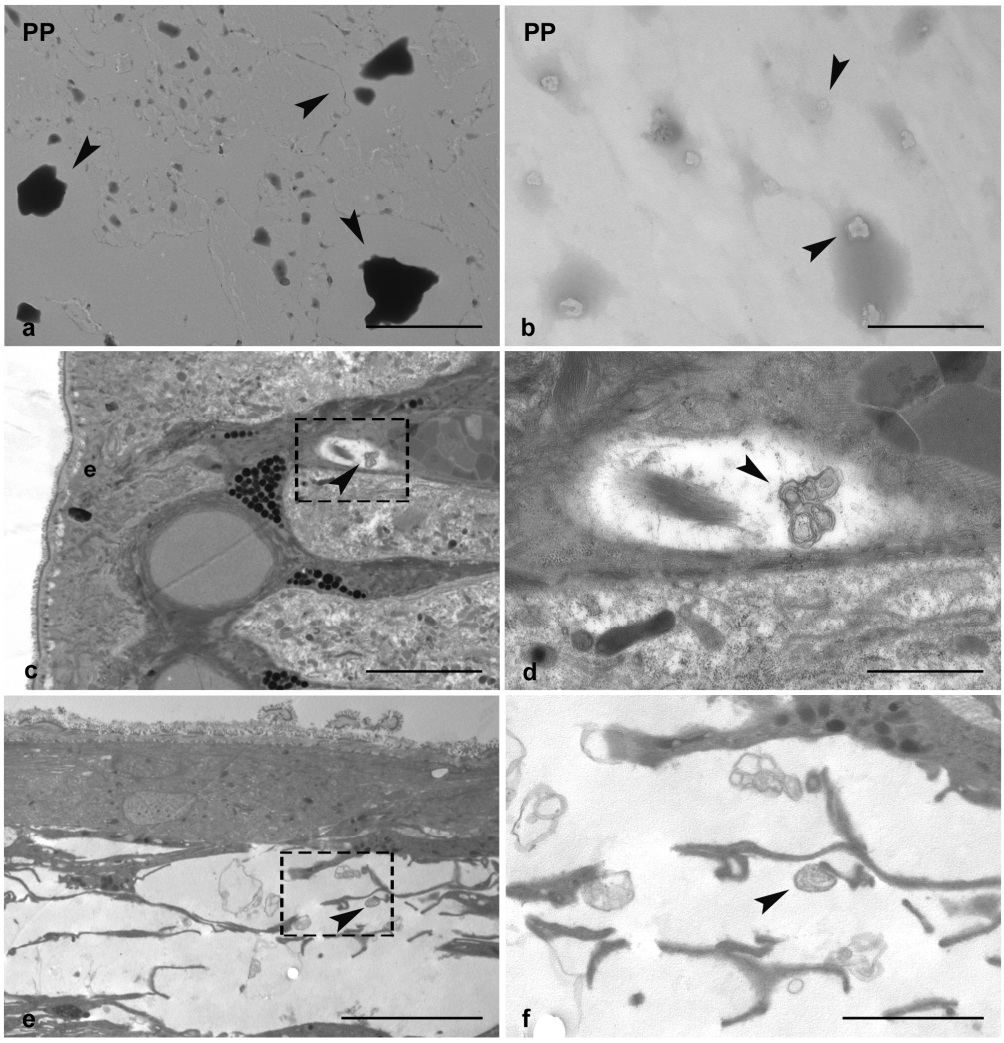

Figure 1. TEM Characterization of PP particles alone (arrowheads in (**a**,**b**)) and internalized in the leech tissue (arrowheads in (**c**–**f**)). In PP-treated injured tissue, NPs aggregates are visible underneath the epithelium (arrowheads in (**c**,**d**)) and in the wound healing area (arrowheads in (**e**,**f**)). Images d and f are details of c and e, respectively, e: epithelium. Bars in (**a**,**c**): 5 µm; (**b**): 500 nm; (**d**): 1 µm; (**e**,**f**): 2.5 µm.

3.2. Morphological Analyses

Morphological analyses were carried out by means of both optical (Figure 2a–h) and transmission electron microscopy (Figure 3a–i). Tissues were examined 24 h, 48 h, 72 h, and 1 w following treatment to assess the effects of PP particles on wound healing and tissue regeneration. In leeches not exposed to plastics, a plug formed by a pseudoblastema was already visible 24 h after injury (Figure 2a). Simultaneously, a newly synthesized

extracellular matrix (ECM) began to flank this structure. Between 48 and 72 h post-injury (Figure 2c,e), the plug became thicker and deeper, filling the entire injured area. A new epithelial layer appeared, creating a protective barrier for the healing tissue against the external environment (Figure 2c). Neo-vessels and clusters of muscle fibers were clearly visible within the ECM (Figure 2a). One week after injury, the wound appeared fully closed, with the muscle layer almost completely restored (Figure 2g). By contrast, after 24 and 48 h post MPs and NPs exposure, the pseudoblastema appeared thinner (Figure 2b,d) and a huge deposition of ECM occurred in the healing area, especially at 72 h and 1 w post-treatment, compared to controls (Figure 2f,h).

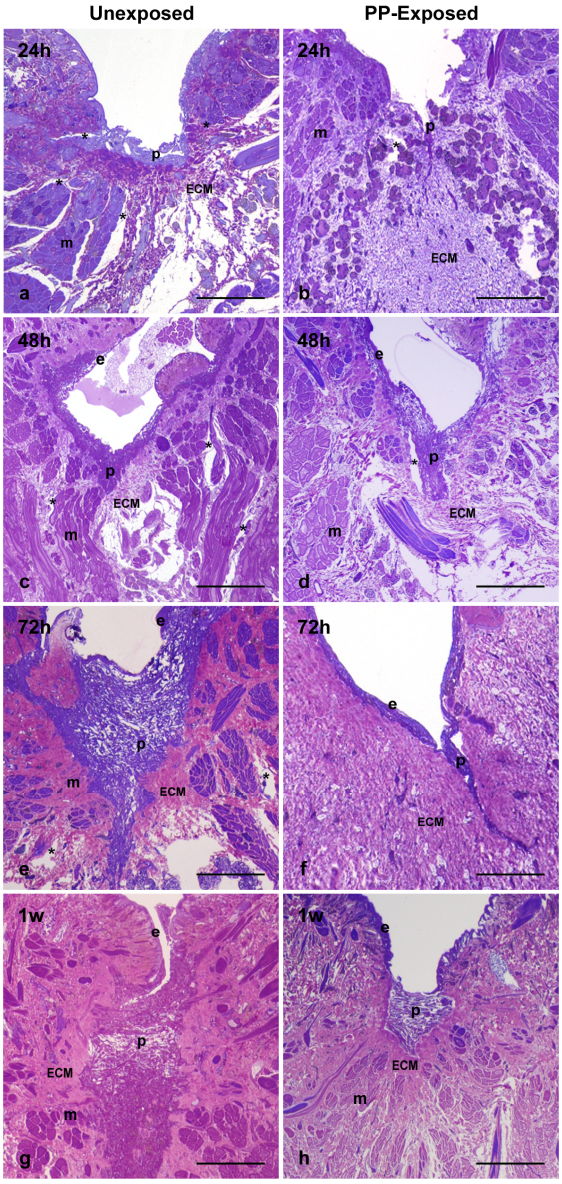

Figure 2. Light microscopy images of injured PP-unexposed (**a**,**c**,**e**,**g**) and PP-exposed leeches (**b**,**d**,**f**,**h**). In PP-unexposed animals, a thick pseudoblastema is visible after 24 h (**a**). A wide plug is observed after 48 h and 72 h (**c**,**e**). New vessels (asterisks in (**a**,**c**,**e**)) and muscle fibers are present in the extracellular matrix. A restored muscle tissue is detectable after 1 w (**g**) in the region adjacent to the thick pseudoblastema. In the injured and PP-exposed leech after 24 h (**b**), a thin pseudoblastema is formed, and few muscle fibers and vessels (v) are visible at 48 h and 72 h (**d**,**f**). After 1 w, a large amount of loose ECM surrounds a thin pseudoblastema (**h**). m: muscle; p: pseudoblastema; ECM: extracellular matrix; e: epithelium. Bars in (**a**–**h**): 100 µm.

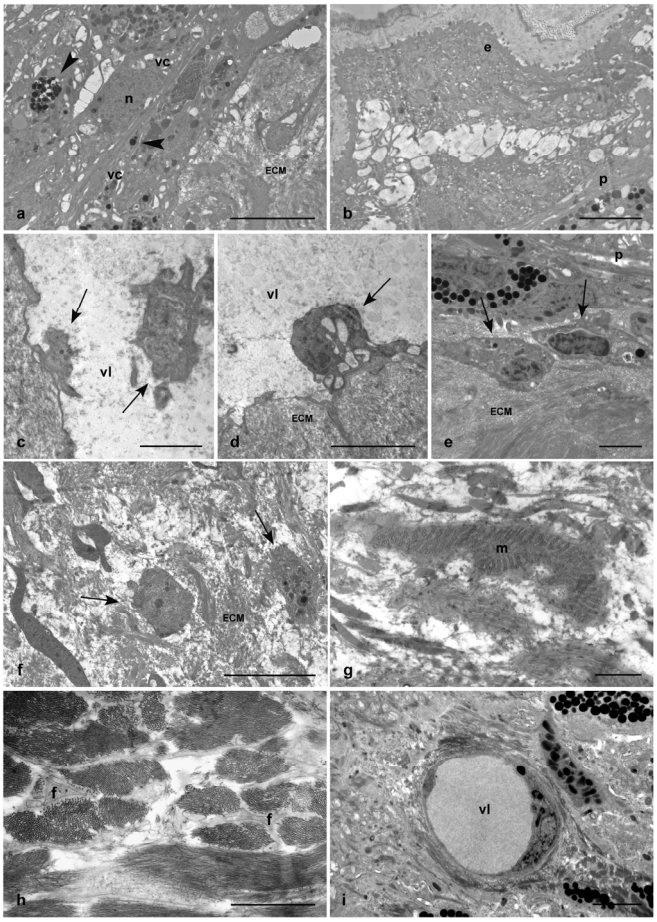

Figure 3. TEM images of injured and PP-unexposed (**a**–**g**) and PP-exposed leeches (**h**,**i**). Detail of packed vasocentral cells organized in parallel rows and characterized by electron-dense cytoplasm containing a few large granules (arrowhead in (**a**)). A newly formed epithelial layer is visible in the wound healing region (**b**). Detail of HSPCs circulating in the vessel lumen (arrows in (**c**)), extravasating (arrows in (**e**)) and localized in the ECM. Star-shaped activated fibroblasts (arrows in (**f**)) and differentiating muscle cells (**g**) are clearly detectable. In injured PP-exposed leeches, a huge amount of ECM is synthesized by numerous star-shaped fibroblasts (**h**). A few neo-vessels not containing HSPCs are present (**i**). ECM: extracellular matrix; n: nucleus; vc: vasocentral cells, m: muscle; vl: vessel lumen; f: fibroblasts. Bars in (**a**,**d**,**i**): 5 µm; bars in (**b**,**c**,**e**,**g**): 2 µm; bars in (**f**,**h**): 1 µm.

Ultrastructural TEM analyses confirmed that, in control samples, the pseudoblastema visible at the edge of the wound was formed by closely packed vasocentral cells, organized in parallel rows and characterized by an electron-dense cytoplasm containing a few large granules (Figure 3a). Moreover, a new epithelial layer could be detected close to this structure, indicating that the re-epithelialization process started (Figure 3b). In addition, Hematopoietic Stem and Progenitor Cells (HSPCs), which normally exploit the neo-vessels synthesis to reach the injured area, were clearly detectable (Figure 3c). These cells extravasated from the bloodstream (Figure 3d) and migrated in the ECM to the regenerating tissues (Figure 3e). In addition, star-shaped activated fibroblasts, characterized by cytoplasmic lamina projections in which new collagen fibril deposition was observable, and tiny differentiating muscle cells, with contractile filaments organized in sarcomeres in the cytoplasm, were observed in the healing region (Figure 3f,g). Of note, in injured and PP-exposed leeches (Figure 3h), only a significant increase in the number of activated fibroblasts was observed, which caused a huge deposition of new collagen fibrils. Furthermore, HSPCs and differentiating muscle fibers were poorly represented, both in the neo-formed vessels and in the newly-laid ECM (Figure 3i).

3.3. Colorimetric Staining of PP-Induced ECM

Collagen-specific Masson's trichrome staining was used to further investigate the effects of PP-MPs and NPs exposure on collagen-based connective tissue remodeling. In the healing area of 72 h injured and PP-unexposed leeches (Figure 4a), a thin and compact collagenous scaffold, surrounding newly formed muscle fiber groups, was visible. By contrast, a remarkable ECM rearrangement occurred after PP exposure. Indeed, 72 h following PP treatment, ECM deposition increased in the healing area (Figure 4b). The pronounced ECM deposition was attributable to the increased number of activated fibroblasts, as previously observed through morphological analyses and further confirmed by total cell counts performed on the same images (Figure 4c). As shown in the graph, the number of fibroblasts increased significantly as early as 24 h after PP exposure, peaked at 72 h, and then declined to baseline levels one week after treatment.

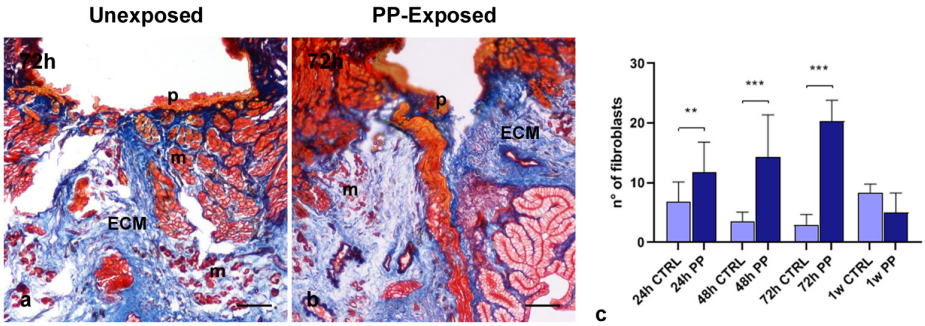

Figure 4. Masson's Trichrome staining and fibroblast count. In 72 h, injured PP-unexposed leeches have a thin and compact ECM (in blue) surrounding newly differentiated muscle fibers (in red) (**a**). In PP-exposed leeches (**b**), a loose ECM bordering the pseudoblastema and containing few muscle cells is visible. The graph (**c**) shows the number of fibroblasts at each time point in PP-unexposed and exposed leech tissue. A significant peak in the fibroblast number occurs in 72 h injured and PP-exposed leeches. Bars in the graphs show the standard deviation (SD) of each mean value, and * represents $p < 0.05$. Significant results are represented as follows: $p < 0.05$ *, $p < 0.01$ **; $p < 0.001$ ***. Statistical analyses refer to the comparison of the same timing samples. p: pseudoblastema; m: muscle; ECM: extracellular matrix. Bars in (**a**,**b**): 100 µm.

3.4. Effect of PP-MPs and NPs on Collagen I, TGF-β and SMAD-3 Expression

To better characterize the newly synthesized ECM during the wound healing process and to evaluate the effect of PP exposure on collagen neo-synthesis, immunofluorescence analyses were performed on leech cryosections (Figure 5a–i). Both injured leeches, untreated (Figure 5a–d) and treated with PP (Figure 5e–h), showed early activation of collagen synthesis (24 h post-treatment), with a rapid increase up to 72 h, followed by a decrease after one week. However, tissues from PP-exposed animals exhibited a noticeably stronger fluorescent signal. No signal was detected in negative controls where the primary antibody was omitted (Figure 5i). The temporal expression profile of COL1-α2 following wounding was evaluated by qPCR analysis (Figure 5j). The results showed an immediate increase in COL1-α2 expression during the early stages of treatment (starting at 24 h post-injury) and continuing up to 72 h. Notably, PP-treated samples exhibited higher expression levels compared to controls. This pattern was further supported by the expression profiles of TGF-β and SMAD-3, two key molecules involved in the collagen pathway, whose expression increased in parallel with COL1-α2, reaching a significant peak at 72 h post-treatment, as illustrated in the graphs (Figure 5k,l).

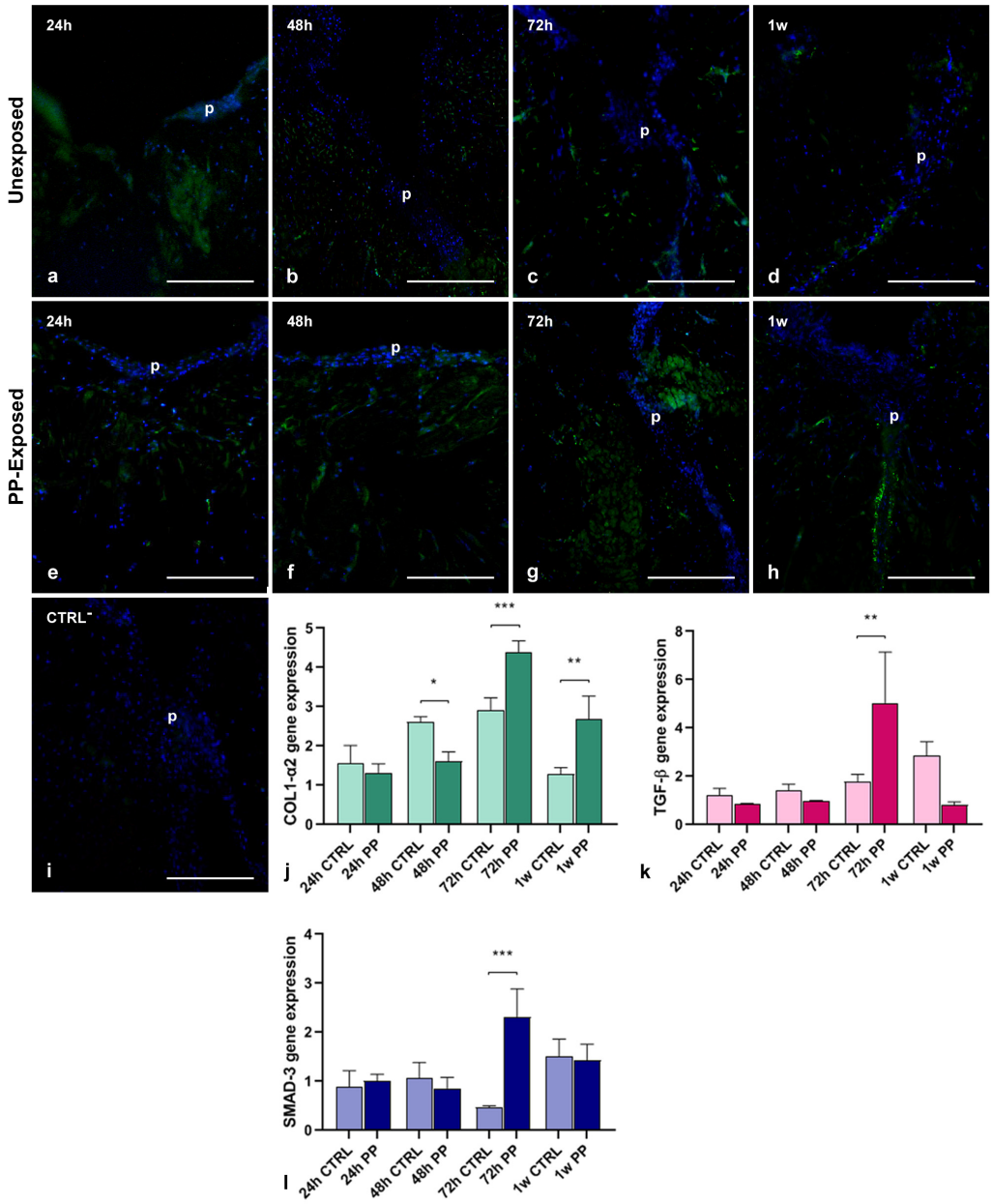

Figure 5. Immunofluorescence and qPCR analyses of injured PP-unexposed and PP-exposed leech tissues. Immunofluorescent analysis of cryosections from control injured PP unexposed (**a**–**d**) and PP-exposed (**e**–**h**) leeches shows that the antibody anti-COL1-α2 stains in green the newly produced collagen fibrils. The green signal is observable starting from 24 h post-injury, increases up to 72 h and remains detectable until 1 w from treatment, with a higher intensity in PP-treated leech tissues. Cell nuclei are stained in blue with DAPI. No signals are detected in negative control experiments (**i**). qPCR analysis (**j**) confirms that COL1-α2 expression profile is coherent with the immunofluorescence analyses. Interestingly, a significant peak of expression at 72 h post-injury is visible in PP-exposed leeches also for TGF-β (**k**) and SMAD3 (**l**). Bars in the graphs show the standard deviation (SD) of each mean value, and * represents $p < 0.05$. Significant results are represented as follows: $p < 0.05$ *, $p < 0.01$ **; $p < 0.001$ ***. Statistical analyses refer to the comparison of the same timing samples. p: pseudoblastema. Bars in (**a**–**i**): 100 µm.

3.5. PP-MPs and NPs Effects on Angiogenesis and Muscle Regeneration

As previously reported, CD34⁺ HSPCs recruited in the healing area by newly-formed vessels represent an important source of myogenic progenitors involved in muscle regeneration [26,27]. However, ultrastructural TEM analyses revealed the presence of HSPCs within the neo-vessels and scattered throughout the connective tissue only in

injured leeches not exposed to PP (Figure 3i), in contrast to those exposed to PP-MPs and NPs.

In order to evaluate whether plastics exposure could impair muscle regeneration by inhibiting both angiogenesis and CD34^{+} HSPCs recruitment in the healing region, immunofluorescent assays and vessel count have been performed. As expected, CD34 expression progressively increased in unexposed control leeches (Figure 6a–d), starting from 24 h and remained high even after one week. By contrast, following exposure to PP (Figure 6e–h), the CD34 signal increased until 48 h and then declined at both 72 h and 1 w post-treatment. No signal was observed in negative control experiments, in which the primary antibody was omitted (Figure 6i). These findings were further supported by quantification of total CD34 fluorescence intensity and vessel count (Figure 6j,k). As shown in the graphs, the reduced CD34 expression correlated with a decreased number of blood vessels in the healing area of PP-exposed injured leeches.

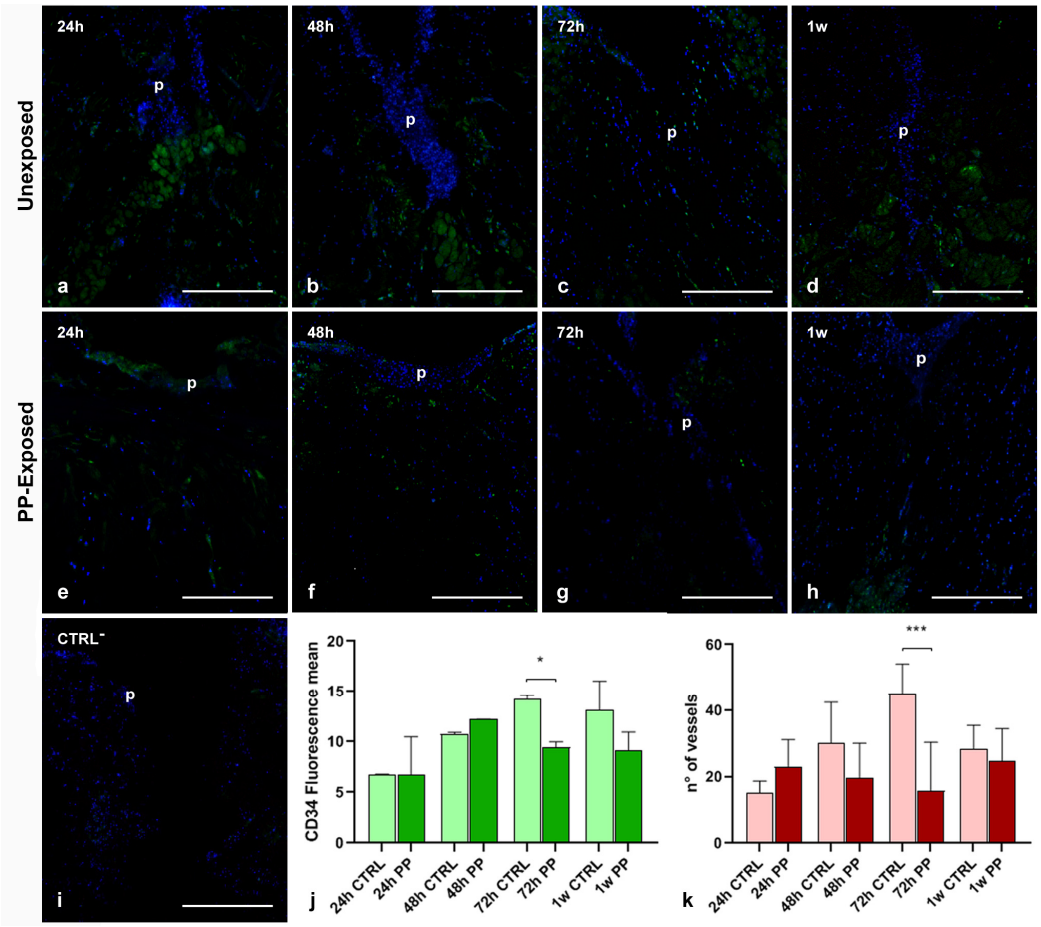

Figure 6. Immunolocalization of CD34+ HSPCs, muscle precursors, and vessel count in the healing region of injured PP-unexposed and PP-exposed leeches. In PP-unexposed leeches, CD34-positive cells are visible at all different timings underneath the pseudoblastema and in the extracellular matrix (ECM) (**a**–**d**). In injured PP-exposed leeches, a low CD34 signal is detectable at 72 h and 1 w (**e**–**h**). Cell nuclei are stained with DAPI. No signals are detected in negative control experiments (**i**). The quantification of CD34 fluorescence signal intensity confirms the trend observed by immunofluorescence assay (**j**). The neo-vessel count graph (**k**) shows a reduced number of vessels starting from 48 h of PP exposure, compared to control injured and PP-unexposed leeches. Bars in the graphs show the standard deviation (SD) of each mean value, and * represents $p < 0.05$. Significant results are represented as follows: $p < 0.05$ *, $p < 0.01$ **; $p < 0.001$ ***. Statistical analyses refer to the comparison of the same timing samples. p: pseudoblastema. Bars in (**a**–**i**): 100 µm.

3.6. Effects of PP-MPs and NPs on Leech Macrophages Recruitment and Tissue Regeneration

In leeches, macrophages are essential cellular components of the innate immune system that play a crucial role not only in the immune response but also in regenerative processes. They phagocyte cellular debris and foreign material, thus preventing the persistence of potentially toxic or immunogenic material in the tissue environment [24]. Furthermore, these cells produce and secrete several molecules such as growth factors, cytokines and enzymes, which are fundamental to induce neo-vessels and immune cells recruitment into the grafted tissues and to promote ECM remodeling or tissue regeneration. Starting from these premises, the effect of PP-MPs and NPs on macrophages phagocytic activity was assessed by the histoenzymatic acid phosphatase (ACP) assay, which selectively stains the lysosomal enzyme of macrophage cells (Figure 7). As expected, after 24 h (Figure 7a,e) and 48 h (Figure 7b,f) from injury, both in control and PP-exposed samples, ACP^+ macrophages appeared in the wounded area, mainly localized in the regenerating sub-epithelial region. These observations are consistent with previous studies, which demonstrated that resident macrophages, responsible for phagocytosis and the encapsulation of pathogens, tissue debris, and nanomaterial particles, were rapidly activated in both unexposed and plastic-exposed samples. On the other hand, following PP exposure, a reduced number of ACP^+ macrophages was visible in the healing area flanking the pseudoblastema after 72 h (Figure 7g) and 1 w (Figure 7h) from injury, compared to control samples (Figure 7c,d). These data, confirmed also by total ACP^+ cell count (Figure 7i), suggested that ACP^+ macrophages recruited after injury may play a crucial role in promoting tissue remodeling processes and that PP exposure could impair their recruitment to the healing area.

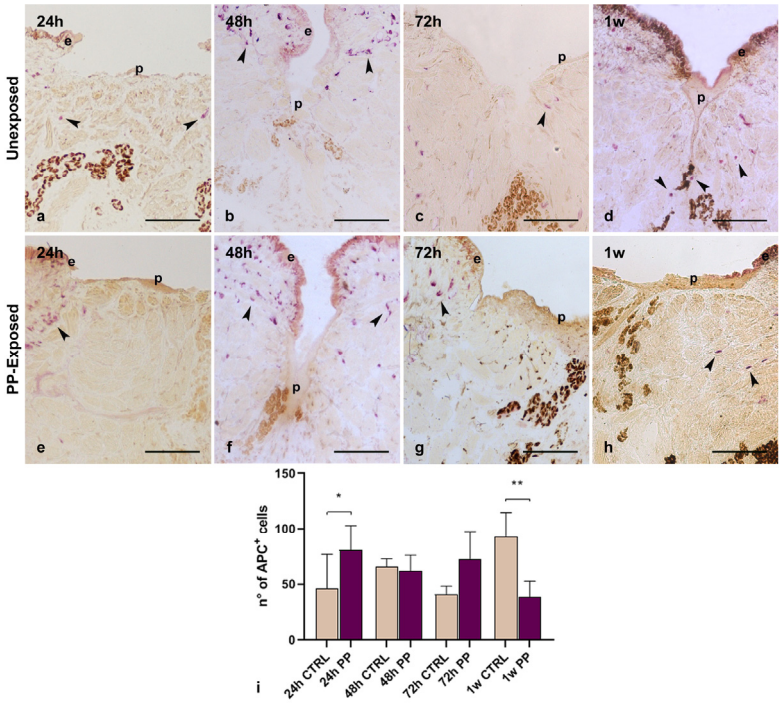

Figure 7. Acid Phosphatase (ACP) histoenzymatic assay. Morphological images of injured PP-unexposed (**a**–**d**) and PP-exposed (**e**–**h**) obtained at the optical light microscope. After 24 h (**a**,**e**) and 48 h (**b**,**f**) from injury, ACP+ macrophages (arrowheads) are mainly localized in the sub-epithelial region. In 72 h (**g**) and 1 w (**h**) injured PP-exposed leeches, few ACP+ macrophages, spread in the wound healing area flanking the pseudoblastema, are visible, compared to injured unexposed samples (**c**,**d**). The graph illustrates the count related to the total number of ACP-positive cells (**i**). Bars in the graphs show the standard deviation (SD) of each mean value, and * represents $p < 0.05$. Significant results are represented as follows: $p < 0.05$ *, $p < 0.01$ **; $p < 0.001$ ***. Statistical analyses refer to the comparison of the same timing samples. Bars in a–h: 100 µm. ECM: extracellular matrix.

3.7. *HvRNASET2 and HmAIF-1 Expression Induced by PP-MPs and NPs*

Leech macrophages carry out critical functions in modulating the innate immune response, fibroplasia and connective tissue remodeling during wound repair through the synthesis of two proteins: the ribonuclease enzyme *Hv*RNASET2 and the pro-inflammatory cytokine *Hm*AIF-1. Starting from these promises, the gene expression levels of these molecules have been evaluated by qPCR analyses to assess how plastics could modulate the functional crosstalk between the inflammatory response and the regenerative process. As shown in the graphs (Figure 8a,b), an increased expression level of these two genes was observed in injured PP-exposed leeches compared to controls. In particular, *HvRNASET2* gene expression increased immediately at 24 h post-treatment, remaining higher in all timings compared to the controls (Figure 8a). By contrast, at 24 h *HmAIF1* was more expressed in injured and PP-unexposed samples, from 48 h to 1 w its synthesis was enhanced (Figure 8b).

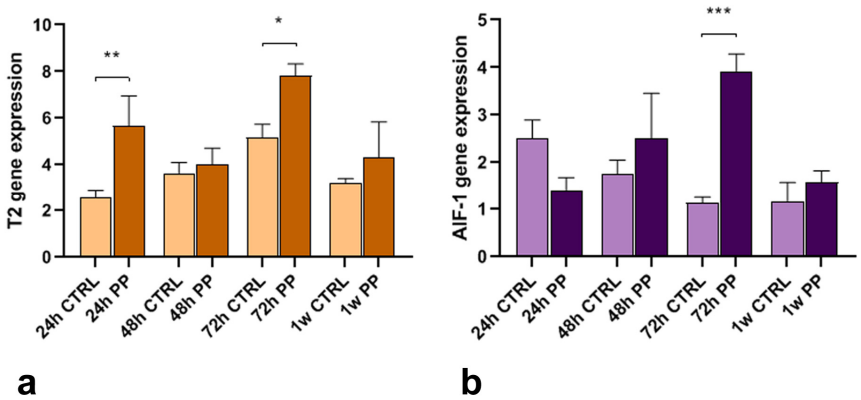

Figure 8. Graphs representing the *Hv*RNASET2 (**a**) and *Hm*AIF-1 (**b**) gene expression analyses, performed by qPCR assays. Compared to injured and PP-unexposed leeches, a peak of both *Hv*RNASET2 and *Hm*AIF-1 factors are detectable in both injured experimental groups at 72 h from treatment. Bars in the graphs show the standard deviation (SD) of each mean value, and * represents $p < 0.05$. Significant results are represented as follows: $p < 0.05$ *, $p < 0.01$ **; $p < 0.001$ ***. Statistical analyses refer to the comparison of the same timing samples.

4. Discussion

Plastic materials have profoundly benefited society, finding applications across various sectors. However, their low degradability, combined with unsustainable use and inadequate waste management, has led to widespread release and accumulation in natural habitats, threatening both aquatic and terrestrial species [30,31]. Although numerous studies highlighted the adverse effects of plastics on wildlife and human health [32], limited data exist on their potential to impair tissue regeneration and wound healing. Notably, the effects of PP-MPs and NPs on these specific processes remain unexplored.

To address these gaps, the medicinal leech *H. verbana* was chosen as a freshwater experimental model. Leeches are increasingly recognized as effective complementary animal models due to their simple anatomy, conservation of cellular and molecular mechanisms, and rapid and straightforward interpretability of results [33]. This study introduces an innovative approach by employing PP films manually minced into MPs and NPs, which mimic debris naturally generated by abiotic and biotic degradation processes. Transmission electron microscopy analyses not only confirmed that these particles, measuring 1–5 µm (MPs) and ~100 nm (NPs), resemble naturally occurring plastic debris [34] but also that they accumulate in leech tissues, particularly under the epithelium and within the connective tissue surrounding muscle fibers. As corroborated by Masson's trichrome staining,

immunofluorescence, and qPCR analyses, this accumulation triggers an inflammatory response that impairs the healing process and muscle regeneration.

Although the precise cellular uptake mechanism of both PP-MPs and NPs in *H. verbana* remains to be fully elucidated, insights from studies on other nanomaterials and invertebrate models suggest multiple possible pathways. For example, it was previously demonstrated that multi-walled carbon nanotubes (MWCNTs) could enter leech cells either through active phagocytosis or by direct membrane piercing, implying that PP-MPs/NPs may exploit similar routes [35].

Given their small size, nanoplastics are also likely to cross epithelial barriers through passive diffusion or receptor-mediated endocytosis. This passage can be facilitated by the formation of an eco-corona, a layer of adsorbed biomolecules on the particle surface, that interacts with scavenger receptors on cell membranes, enhancing internalization. Once inside the organism, these particles may accumulate in tissues, triggering inflammatory and fibrotic responses similar to those documented in our leech model and other invertebrates [36,37]. To precisely define the cellular uptake routes of PP-MPs/NPs in *H. verbana*, further investigations combining advanced imaging techniques, molecular markers of endocytosis and phagocytosis, and functional assays examining immune responses are essential. Such multidisciplinary approaches will clarify whether these particles primarily enter via active cellular processes, passive diffusion, or a combination of mechanisms, providing a clearer understanding of their biological impact in aquatic invertebrates.

As previously demonstrated in leeches, the interplay between immune response and tissue regeneration is crucial for effective healing [33]. Indeed, macrophage-like cells in leech, as in vertebrates [38,39], play a dual role in host defense and tissue repair. On one side, they clear pathogens and debris, and on the other side, they mediate ECM remodeling and tissue repair through the secretion of cytokines and enzymes such as *Hm*AIF-1 and *Hv*RNASET2, which in turn regulate immune cell recruitment, fibroblast activation, collagen deposition, and angiogenesis [40]. However, a prolonged or excessive inflammation can lead to fibrosis, characterized by excessive ECM deposition. This imbalance limits angiogenesis and the delivery of $CD34^+$ myoendothelial muscle precursors to the injured site, impairing muscle fiber regeneration [26]. Of note, after 72 h of exposure to PP-MPs and NPs, the significant presence of ACP^+ macrophage-like cells coincide with elevated levels of *Hm*AIF-1 and *Hv*RNASET2 expression, as well as increased *TGF-β* and *SMAD3* expression. This observation confirms the role of these two factors, already described in vertebrates, in mediating inflammatory responses and remodeling connective tissue during tissue regeneration [41]. In addition, in vertebrates, the release and activation of TGF-β, mediated through its associated SMAD3 signaling pathway, stimulate the production of various ECM proteins while simultaneously inhibiting their degradation. These actions of TGF-β are crucial for tissue repair, as they ideally facilitate the restoration of normal tissue architecture and function. However, when TGF-β activity becomes excessive, it can result in pathological fibrosis, characterized by abnormal ECM deposition that disrupts the normal wound-healing process [42,43]. Indeed, in vertebrates, fibroblasts derived from hypertrophic scars and hypertrophic scar tissue exhibit significantly higher expression of TGF-β mRNA and related proteins, compared to fibroblasts from normal skin, highlighting the critical role of TGF-β in the development of hypertrophic scars and suggesting its involvement in pathological fibrosis [44].

These data suggest that, as in vertebrates [45–47], following the ingestion of nanomaterials or the presence of cellular debris, leech macrophage-like cells produce high levels of TGF-β and SMAD3, which in turn cause the development of fibrosis and the consequent overproduction of collagen. Ultrastructural analysis by TEM supports this hypothesis, revealing numerous activated spindle-shaped fibroblasts actively involved in extensive col-

lagen production and reorganization, especially in wounded samples exposed to a mixture of PP-MPs and NPs for 72 h.

5. Conclusions

The current study provides a comprehensive analysis of the effects of polypropylene micro- and nanoparticles on wound healing and tissue regeneration in leeches, highlighting the complex interplay between extracellular matrix remodeling, immune cell recruitment, and angiogenesis. Our results reveal that exposure to PP-MPs and NPs significantly alters the natural wound healing process by increasing ECM deposition, mainly driven by an upregulation of activated fibroblasts. Although this mechanism may initially support structural repair, it appears to subsequently interfere with the HSPCs recruitment and the formation of new blood vessels, potentially compromising muscle regeneration and tissue function. These findings also demonstrate that PP interferes with the modulation of the expression of key genes involved in collagen synthesis, such as COL1-α2, TGF-β, and SMAD-3, with a peak of expression especially observed at 72 h after treatment. Furthermore, macrophage-like cell recruitment appears significantly reduced at later time points, revealing a compromised immune response that could further impede proper tissue remodeling.

These findings emphasize the potential detrimental impact of environmental pollutants, such as PP-MPs and NPs, on biological systems. By impairing critical processes like angiogenesis, muscle regeneration, and immune cell recruitment, plastic particles affect tissue repair mechanisms, raising concerns about their long-term effects on ecosystem health and stability. Future studies should aim to elucidate the molecular pathways underlying these disruptions and investigate potential mitigation strategies to counteract the negative effects of plastic pollution on living organisms. This knowledge is crucial to understanding and managing the broader implications of micro- and nanoplastics contamination in the environment.

It is important to note that our conclusions refer specifically to the leech model, and any potential implications for vertebrate biology are considered solely within the framework of conserved molecular pathways, with appropriate limitations clearly acknowledged. This cautious approach avoids over-interpretation while highlighting the evolutionary parallels that can inform future translational research.

Supplementary Materials: The following supporting information can be downloaded at: https://www.mdpi.com/article/10.3390/microplastics4030056/s1, Figure S1: 13C NMR spectrum of the i-PP sample (TCDE solvent, HMDS scale, 100 °C); Figure S2: 1H NMR spectrum of the i-PP sample (TCDE solvent, HMDS scale, 100 °C); Figure S3: GPC trace of the i-PP sample; Figure S4: TGA trace of the i-PP sample; Figure S5: DSC curves (second heating run) of the i-PP sample; Figure S6: X ray diffraction pattern of the i-PP sample; Table S1: List of primers used for qPCR analyses; Table S2: List of mean values related to fibroblasts' count; Table S3: List of mean values related to COLI-α2 expression; Table S4: List of mean values related to TGF-β expression; Table S5: List of mean values related to SMAD-3 expression; Table S6: List of mean values related to CD34 fluorescence intensity; Table S7: List of mean values related to blood vessel's count; Table S8: List of mean values related to ACP^+ cells count; Table S9: List of mean values related to *Hv*RNASET2 gene expression; Table S10: List of mean values related to *Hm*AIF-1 gene expression.

Author Contributions: C.B.: Formal analysis, Investigation, Writing—review and editing. A.M. Formal analysis, Investigation, Writing—review and editing. L.P.: Formal analysis, Investigation, Validation, Writing—review and editing. N.P.: Formal analysis, Investigation, Writing—review and editing. O.S.: Formal analysis, Methodology, Supervision; Writing—review and editing. S.P.: Formal analysis, Methodology, Supervision; Writing—review and editing. L.I.: Formal analysis, Methodology, Supervision; Validation; Writing—review and editing. N.B.: Formal analysis, Funding

Acquisition, Supervision; Validation; Writing—original draft. A.G.: Conceptualization, Funding Acquisition, Project administration, Supervision, Validation, Writing—original draft. All authors have read and agreed to the published version of the manuscript.

Funding: This research was funded by PRIN (Progetti di Ricerca di rilevante Interesse Nazionale), grant number 2022SAHTRX by A.G. and by FAR (Fondo di Ateneo per la Ricerca) by A.G. and N.B.

Institutional Review Board Statement: As reported in the text "The use of the leech H. verbana is not among the animals protected under Directive 2010/63/EU, which governs the use of animals in scientific research, nor is it listed in Legislative Decree no. 26, of 4 March 2014, "Implementing Directive 2010/63/EU on the protection of animals used for scientific purposes", published in the Italian Official Journal on 14 March 2014. However, its use has been approved by the Animal Welfare Body (OPBA) at the University of Insubria, and it complies with the commonly accepted '3Rs".

Data Availability Statement: The data presented in this study are available in the article and Supplementary Materials.

Acknowledgments: C.B. is a PhD student of Life Sciences and Biotechnology course at University of Insubria. Scientific support from CRIETT center of University of Insubria (instrument code MIC01) is greatly acknowledged.

Conflicts of Interest: The authors declare no conflicts of interest.

Abbreviations

The following abbreviations are used in this manuscript:

ACP	Acid Phosphatase
ANOVA	Analysis of Variance
BSA	Bovine Serum Albumin
COL1-α2	Collagen Type I Alpha 2 Chain
DAPI	4′,6-Diamidino-2-Phenylindole
ECM	Extracellular Matrix
FITC	Fluorescein Isothiocyanate
GAPDH	Glyceraldehyde-3-Phosphate Dehydrogenase
*Hm*AIF-1	*Hirudo medicinalis* Allograft Inflammatory Factor-1
HSPCs	Hematopoietic Stem and Progenitor Cells
*Hv*NASET2	*Hirudo verbana* Ribonuclease T2
MPs	Microplastics
NMR	Nuclear Magnetic Resonance
NPs	Nanoplastics
OsO_4	Osmium Tetroxide
PBS	Phosphate Buffered Saline
PP	Polypropylene
qPCR	Quantitative PCR (Polymerase Chain Reaction)
SEC	Size Exclusion Chromatography
SD	Standard Deviation
TEM	Transmission Electron Microscopy
TGF-β	Transforming Growth Factor Beta

References

1. Hahladakis, J.N.; Velis, C.A.; Weber, R.; Iacovidou, E.; Purnell, P. An overview of chemical additives present in plastics: Migration, release, fate and environmental impact during their use, disposal and recycling. *J. Hazard. Mater.* **2018**, *344*, 179–199. [CrossRef]
2. Chandran, M.; Tamilkolundu, S.; Murugesan, C. Characterization studies: Waste plastic oil and its blends Characterization studies: Waste plastic oil and its blends. *Energy Sources Part A* **2019**, *42*, 281–291. [CrossRef]
3. Sigler, M. The Effects of Plastic Pollution on Aquatic Wildlife: Current Situations and Future Solutions. *Water Air Soil Pollut.* **2014**, *225*, 2184. [CrossRef]

4. Yee, M.S.; Hii, L.; Looi, C.K.; Lim, W.; Wong, S.; Kok, Y.; Tan, B.; Wong, C.; Leong, C. Impact of Microplastics and Nanoplastics on Human Health. *Nanomaterials* **2021**, *11*, 496. [CrossRef]
5. Yang, L.; Zhang, Y.; Kang, S.; Wang, Z.; Wu, C. Science of the Total Environment Microplastics in freshwater sediment: A review on methods, occurrence, and sources. *Sci. Total Environ.* **2021**, *754*, 141948. [CrossRef] [PubMed]
6. Wagner, M.; Scherer, C.; Alvarez-muñoz, D.; Brennholt, N.; Bourrain, X.; Buchinger, S.; Fries, E.; Grosbois, C.; Klasmeier, J.; Marti, T.; et al. Microplastics in freshwater ecosystems: What we know and what we need to know. *Environ. Sci. Eur.* **2014**, *26*, 12. [CrossRef] [PubMed]
7. Au, S.Y.; Bruce, T.F.; Bridges, W.C.; Klaine, S.J. Responses of Hyalella azteca to acute and chronic microplastic exposures. *Environ. Toxicol. Chem.* **2015**, *34*, 2564–2572. [CrossRef]
8. Barrick, A.; Boardwine, A.J.; Nguyen, N.H.A.; Sevcu, A.; Novotna, J.; Hoang, T.C. Acute toxicity of natural and synthetic clothing fibers towards Daphnia magna: Influence of fiber type and morphology. *Sci. Total Environ.* **2025**, *967*, 178751. [CrossRef]
9. Engler, R.E. Chemicals in the Ocean. *Environ. Sci. Technol.* **2012**, *46*, 302–315. [CrossRef]
10. Gu, L.; Tian, L.; Gao, G.; Peng, S.; Zhang, J.; Wu, D.; Huang, J.; Hua, Q.; Lu, T.; Zhong, L.; et al. Inhibitory effects of polystyrene microplastics on caudal fin regeneration in zebrafish larvae. *Environ. Pollut.* **2020**, *266*, 114664. [CrossRef]
11. Maddah, H.A. Polypropylene as a Promising Plastic: A Review. *Am. J. Polym. Sci.* **2016**, *6*, 1–11. [CrossRef]
12. Wang, Z.; Zhang, Y.; Kang, S.; Yang, L.; Shi, H.; Tripathee, L.; Gao, T. Research progresses of microplastic pollution in freshwater systems. *Sci. Total Environ.* **2021**, *795*, 148888. [CrossRef]
13. Raddadi, N.; Fava, F. Biodegradation of oil-based plastics in the environment: Existing knowledge and needs of research and innovation. *Sci. Total Environ.* **2019**, *679*, 148–158. [CrossRef]
14. Mohan, P.; Shahul, F. Charting the microplastic menace: A bibliometric analysis of pollution in *Malaysian mangroves* and polypropylene bioaccumulation assessment in *Anadara granosa*. *Mar. Pollut. Bull.* **2024**, *205*, 116654. [CrossRef]
15. Shahul Hamid, F.; Bhatti, M.S.; Anuar, N.; Anuar, N.; Mohan, P.; Periathamby, A. Worldwide distribution and abundance of microplastic: How dire is the situation? *Waste Manag. Res.* **2018**, *36*, 873–897. [CrossRef]
16. Jahan, I.; Chowdhury, G.; Rafi, S.; Ashab, A.; Sarker, M.; Chakraborty, A.; Couetard, N.; Anamul, M.; Hossain, A.; Mahbub, M. Assessment of dietary polyvinylchloride, polypropylene and polyethylene terephthalate exposure in *Nile tilapia*, *Oreochromis niloticus*: Bioaccumulation, and effects on behaviour, growth, hematology. *Environ. Pollut.* **2024**, *345*, 123548. [CrossRef] [PubMed]
17. Thomas, P.J.; Perono, G.; Tommasi, F.; Pagano, G.; Oral, R.; Buri, P.; Kova, I.; Toscanesi, M.; Trifuoggi, M.; Lyons, D.M. Resolving the effects of environmental micro- and nanoplastics exposure in biota: A knowledge gap analysis. *Sci. Total Environ.* **2021**, *780*, 146534. [CrossRef]
18. Montero, D.; Rimoldi, S.; Torrecillas, S.; Rapp, J.; Moroni, F.; Herrera, A.; Gómez, M.; Fernández-montero, Á.; Terova, G. Impact of polypropylene microplastics and chemical pollutants on European sea bass (*Dicentrarchus labrax*) gut microbiota and health. *Sci. Total Environ.* **2022**, *805*, 150402. [CrossRef] [PubMed]
19. Baranzini, N.; Pulze, L.; Bon, C.; Izzo, L.; Pragliola, S.; Venditto, V.; Grimaldi, A. Hirudo verbana as a freshwater invertebrate model to assess the effects of polypropylene micro and nanoplastics dispersion in freshwater. *Fish Shellfish Immunol.* **2022**, *127*, 492–507. [CrossRef] [PubMed]
20. Cheng, Y.; Song, W.; Tian, H.; Zhang, K.; Li, B.; Du, Z.; Zhang, W.; Wang, J.; Wang, J.; Zhu, L. Chemosphere The effects of high-density polyethylene and polypropylene microplastics on the soil and earthworm *Metaphire guillelmi* gut microbiota. *Chemosphere* **2021**, *267*, 129219. [CrossRef]
21. Gambino, G.; Falleni, A.; Nigro, M.; Salvetti, A.; Cecchettini, A.; Ippolito, C.; Guidi, P.; Rossi, L. Dynamics of interaction and effects of microplastics on planarian tissue regeneration and cellular homeostasis. *Aquat. Toxicol.* **2020**, *218*, 105354. [CrossRef]
22. Gao, T.; Sun, B.; Xu, Z.; Chen, Q.; Yang, M.; Wan, Q.; Song, L.; Chen, G.; Jing, C.; Zeng, E.Y.; et al. Exposure to polystyrene microplastics reduces regeneration and growth in planarians. *J. Hazard. Mater.* **2022**, *432*, 128673. [CrossRef]
23. Leung, J.; Chan, K.Y.K. Microplastics reduced posterior segment regeneration rate of the polychaete *Perinereis aibuhitensis*. *Mar. Pollut. Bull.* **2018**, *129*, 782–786. [CrossRef]
24. Pragliola, S.; Grisi, F.; Vitale, V.; Sacco, O.; Venditto, V.; Izzo, L.; Grimaldi, A.; Baranzini, N. New fluorescence labeling isotactic polypropylenes as a tracer: A proof of concept. *Polym. Chem.* **2022**, *13*, 2685–2693. [CrossRef]
25. Pulze, L.; Baranzini, N.; Congiu, T.; Acquati, F.; Grimaldi, A. Spatio-Temporal Changes of Extracellular Matrix (ECM) Stiffness in the Development of the Leech *Hirudo verbana*. *Int. J. Mol. Sci.* **2022**, *23*, 5953. [CrossRef]
26. Baranzini, N.; Pulze, L.; Tettamanti, G.; Acquati, F.; Grimaldi, A. HvRNASET2 Regulate Connective Tissue and Collagen I Remodeling During Wound Healing Process. *Front. Physiol.* **2021**, *12*, 632506. [CrossRef]
27. Grimaldi, A.; Banfi, S.; Gerosa, L.; Tettamanti, G.; Noonan, D.M.; Valvassori, R.; de Eguileor, M. Identification, isolation and expansion of myoendothelial cells involved in leech muscle regeneration. *PLoS ONE* **2009**, *4*, e7652. [CrossRef] [PubMed]
28. Untergasser, A.; Cutcutache, I.; Koressaar, T.; Ye, J.; Faircloth, B.C.; Remm, M.; Rozen, S.G. Primer3-new capabilities and interfaces. *Nucleic Acids Res.* **2012**, *40*, e115. [CrossRef] [PubMed]

29. Schwabl, P.; Köppel, S.; Königshofer, P.; Bucsics, T.; Trauner, M.; Reiberger, T.; Liebmann, B. Detection of Various Microplastics in Human Stool: A Prospective case series. *Ann. Intern. Med.* **2019**, *171*, 453–457. [CrossRef]
30. Bilal, M.; Iqbal, H.M.N. Transportation fate and removal of microplastic pollution—A perspective on environmental pollution. *Case Stud. Chem. Environ. Eng.* **2020**, *2*, 100015. [CrossRef]
31. Morrison, M.; Trevisan, R.; Ranasinghe, P.; Merrill, G.B.; Santos, J.; Hong, A.; Edward, W.C.; Jayasundara, N.; Somarelli, J.A. A growing crisis for One Health: Impacts of plastic pollution across layers of biological function. *Front. Mar. Sci.* **2022**, *9*, 980705. [CrossRef]
32. Kukkola, A.; Krause, S.; Lynch, I.; Sambrook Smith, G.H.; Nel, H. Nano and microplastic interactions with freshwater biota—Current knowledge, challenges and future solutions. *Environ. Int.* **2021**, *152*, 106504. [CrossRef]
33. Baranzini, N.; Pulze, L.; Acquati, F.; Grimaldi, A. Hirudo verbana as an alternative model to dissect the relationship between innate immunity and regeneration. *Invertebr. Surviv. J.* **2020**, *17*, 90–98.
34. Fu, W.; Min, J.; Jiang, W.; Li, Y.; Zhang, W. Separation, characterization and identification of microplastics and nanoplastics in the environment. *Sci. Total Environ.* **2020**, *721*, 137561. [CrossRef]
35. Girardello, R.; Tasselli, S.; Baranzini, N.; Valvassori, R.; De Eguileor, M.; Grimaldi, A. Effects of carbon nanotube environmental dispersion on an aquatic invertebrate, Hirudo medicinalis. *PLoS ONE* **2015**, *10*, e0144361. [CrossRef] [PubMed]
36. Bodó, K.; Baranzini, N.; Girardello, R.; Kokhanyuk, B.; Németh, P.; Hayashi, Y.; Grimaldi, A.; Engelmann, P. Nanomaterials and annelid immunity: A comparative survey to reveal the common stress and defense responses of two sentinel species to nanomaterials in the environment. *Biology* **2020**, *9*, 307. [CrossRef]
37. Yang, H.; Chen, Z.; Kong, L.; Xing, H.; Yang, Q.; Wu, J. A Review of Eco-Corona Formation on Micro/Nanoplastics and Its Effects on Stability, Bioavailability, and Toxicity. *Water* **2025**, *17*, 1124. [CrossRef]
38. Bohaud, C.; Johansen, M.D.; Jorgensen, C.; Ipseiz, N.; Kremer, L.; Djouad, F. The Role of Macrophages During Zebrafish Injury and Tissue Regeneration Under Infectious and Non-Infectious Conditions. *Front. Immunol.* **2021**, *12*, 707824. [CrossRef]
39. Mescher, A.L. Macrophages and fibroblasts during inflammation and tissue repair in models of organ regeneration. *Regeneration* **2017**, *4*, 39–53. [CrossRef] [PubMed]
40. Baranzini, N.; De Vito, A.; Orlandi, V.T.; Reguzzoni, M.; Monti, L.; de Eguileor, M.; Rosini, E.; Pollegioni, L.; Tettamanti, G.; Acquati, F.; et al. Antimicrobial Role of RNASET2 Protein During Innate Immune Response in the Medicinal Leech *Hirudo verbana*. *Front. Immunol.* **2020**, *11*, 370. [CrossRef]
41. Seo, D.; Hare, J.M. The transforming growth factor-β/Smad3 pathway: Coming of age as a key participant in cardiac remodeling. *Circulation* **2007**, *116*, 2096–2098. [CrossRef]
42. Branton, M.H.; Kopp, J.B. TGF-β and fibrosis. *Microbes Infect.* **1999**, *1*, 1349–1365. [CrossRef]
43. Mack, M. Inflammation and fibrosis. *Matrix Biol.* **2018**, *68–69*, 106–121. [CrossRef]
44. Penn, J.W.; Grobbelaar, A.O.; Rolfe, K.J. The role of the TGF—β family in wound healing, burns and scarring: A review. *IJBT* **2012**, *2*, 18–28.
45. Nacu, N.; Luzina, I.G.; Highsmith, K.; Pochetuhen, K.; Cooper, Z.A.; Michael, P.; Todd, N.W.; Atamas, S.P.; Lockatell, V.; Gillmeister, M.P.; et al. Macrophages Produce TGF-β-Induced (β-ig-h3) following Ingestion of Apoptotic Cells and Regulate MMP14 Levels and Collagen Turnover in Fibroblasts. *J. Immunol.* **2008**, *180*, 5036–5044. [CrossRef]
46. Vannella, K.M.; Wynn, T.A. Mechanisms of Organ Injury and Repair by Macrophages∗. *Annu. Rev. Physiol.* **2017**, *79*, 593–617. [CrossRef] [PubMed]
47. Wynn, T.A.; Vannella, K.M. Macrophages in Tissue Repair, Regeneration, and Fibrosis. *Immunity* **2016**, *44*, 450–462. [CrossRef] [PubMed]

Disclaimer/Publisher's Note: The statements, opinions and data contained in all publications are solely those of the individual author(s) and contributor(s) and not of MDPI and/or the editor(s). MDPI and/or the editor(s) disclaim responsibility for any injury to people or property resulting from any ideas, methods, instructions or products referred to in the content.